

# Revisiting and Modeling Power-Law Distributions in Empirical Outage Data of Power Systems


Bálint Hartmann<sup>1,\*</sup>, Shengfeng Deng<sup>2,†</sup>, Géza Ódor<sup>2</sup>, and Jeffrey Kelling<sup>3,4</sup>

<sup>1</sup>*Institute of Energy Security and Environmental Safety, Center for Energy Research, P.O. Box 49, Budapest H-1525, Hungary*

<sup>2</sup>*Institute of Technical Physics and Materials Science, Center for Energy Research, P.O. Box 49, Budapest H-1525, Hungary*

<sup>3</sup>*Faculty of Natural Sciences, Chemnitz University of Technology, Straße der Nationen 62, Chemnitz 09111, Germany*

<sup>4</sup>*Department of Information Services and Computing, Helmholtz-Zentrum Dresden-Rossendorf, P.O.Box 51 01 19, Dresden 01314, Germany*

 (Received 27 March 2023; revised 19 June 2023; accepted 10 July 2023; published 4 August 2023)

The size distributions of planned and forced outages and their restoration times in power systems have been studied for almost two decades and have drawn great interest as they display heavy tails. Understanding heavy tails has been provided by various threshold models, which are self-tuned at their critical points, but as many papers pointed out, explanations are intuitive, and more empirical data are needed to support hypotheses. In this paper, we analyze outage data collected from various public sources to calculate the outage energy and outage duration exponents of possible power-law fits. Temporal thresholds are applied to identify crossovers from initial short-time behavior to power-law tails. We revisit and add to the possible explanations of the uniformness of these exponents. By performing power spectral analyses on the outage event time series and the outage duration time series, we find that, on the one hand, while being overwhelmed by white noise, outage events show traits of self-organized criticality, which may be modeled by a crossover from random percolation to a directed percolation branching process with dissipation, coupled to a conserved density. On the other hand, in response to outages, the heavy tails in outage duration distributions could be a consequence of the highly optimized tolerance mechanism, based on the optimized allocation of maintenance resources.

DOI: [10.1103/PRXEnergy.2.033007](https://doi.org/10.1103/PRXEnergy.2.033007)

## I. INTRODUCTION

As the power sector undergoes an unprecedented transition, understanding the vulnerability of these systems receives more attention from the research community. Replacing conventional, dominantly fossil-fueled power plants with ones relying on variable sources such as solar and wind poses a number of challenges, mainly due to the appearing correlated spatiotemporal fluctuations, which in case of adverse conditions can lead to disturbances of various sizes. The size distribution of such events has been the focus of research for almost two decades, largely because

it displays fat tails; a suitable candidate for fitting power laws. It is known that the severity of catastrophic events exhibits such behavior, even after removing extreme outliers [1,2]. The probability distribution of the number of people killed in natural disasters and man-made situations also shows power-law decay, with very similar exponent values. As presented in Ref. [3], the size distribution of deaths in man-made events (wars, battles, conflicts, terrorist attacks) decays with power-law tails, with exponents around 1.6. Similarly, the magnitudes of natural disasters (earthquakes, storms, wildfires, etc.) show exponents between 1.8 and 1.5. If such extreme events do follow a power law, they are not completely unexpected anymore; though they remain unpredictable. (These events were coined by Taleb as “gray swans” [4], in contrast to “black swans,” which can still occur due to the possible dynamics of the upper cutoff [5].)

The research community is actively working on the improvement of our understanding on how power outages can be forecasted [6] and, more specifically, whether

\*hartmann.balint@ek-cer.hu

†shengfeng.deng@ek-cer.hu

*Published by the American Physical Society under the terms of the [Creative Commons Attribution 4.0 International](https://creativecommons.org/licenses/by/4.0/) license. Further distribution of this work must maintain attribution to the author(s) and the published article's title, journal citation, and DOI.*

the risk of failure in power systems represents a specific case of the risk of system-wide breakdown in threshold-activated disordered systems. Self-organized criticality (SOC), explained first by the Bak-Tang-Wiesefeld model [7], is widely used for the modeling of such phenomena [8]. In this regard, SOC is expected as the consequence of self-tuning to a critical point, which is determined by the competition of power consumption (behavioral properties) and available transmission capabilities (infrastructural properties) of the examined power system. In the early 2000s, another model gained some attention in relation to the topic, namely, the highly optimized tolerance (HOT) model. HOT was coined by Carlson and Doyle, claiming that the model takes into consideration the fact that designs are developed and biological systems evolve in a manner that rewards successful strategies subject to a specific form of external stimulus [9]. Following this original paper, Stubna and Fowler [10] examined the HOT model using data from the Western United States and concluded that the model agrees closely if the outage event size is considered through the power loss but not for the number of consumers affected; thus, the model of optimal resource distribution is not valid in general when more than one measure of the event size is used. They also suggested a modified model, which introduces the misallocation of resources. Lin and Bo [11] showed similar findings that the HOT model is not a generic one that can be used for applications related to power systems, but it was worth studying the model as a tool of power system blackout mechanism analysis and countermeasure. It was also shown in Ref. [12] that the HOT mechanism can also replicate empirical statistics of power outages. It has to be noted that dimensions of the grid are critical for HOT predictions, as they determine the exponent. Calculating the dimensions of power grids is challenging due to their complex topology, but in general the graph dimension of high-voltage networks is considered to be over 2 [13]. An interesting point raised by Hohensee [12] is that, while both the SOC and HOT models can replicate the size distributions of outages, the main difference might be seen in the temporal correlation of the events, with which SOC could manifest a  $1/f^\alpha$  noise [14,15]. However, previously studied data still cover a too short time span, restricting one to assert, in typical power systems, if it is SOC or HOT in play or an interplay of both.

By studying more outage data from various sources and time spans, this latter argument served as one of the main motivations for our paper, as we revisit the empirical studies carried out in the last two decades, and perform an in-depth comparison with our recent findings.

When reviewing the corresponding literature, one has to pay attention to the adequate use of the terminology, especially when comparing outages, restorations, and blackouts. While the size and duration of blackouts are characteristic properties of the power system under study,

outages caused by component failure are typically individual events. As shown by Dobson and Ekisheva [16], the duration of outages is usually much shorter than that of blackouts and their restorations, and large blackouts, albeit rare, are much more hazardous to society [17,18]. One also has to differentiate the type of component leading to the outage; repairs for generation equipment and transmission equipment not only differ in their nature but also in their duration. Generation outages are caused by failure of the machinery at a single site, while transmission outages can occur at multiple locations and are also subject to weather.

For blackouts, the first widely analyzed dataset was the probability distribution of unserved energy in relation to North American blackouts between 1984 and 1998 [19], which showed a power-law-like tail [8,20] with a decay exponent between 1.3 and 2.0. Blackout statistics along the dimension of energy were analyzed for New Zealand [21] (exponent approximately 1.6) and China [22] (1.8), while for the dimension of power, data for North America [20,23] (2.0) and Norway [24] (1.7) were analyzed earlier. Disturbance data of Sweden were analyzed in Ref. [25] (exponent approximately 1.6). Besides these examples of empirical data, various power system models are also used to study SOC processes; the most relevant being the standard blackout model named ORNL-PSerc-Alaska (OPA). The OPA model was also validated for real-world data in Ref. [26].

Those previous data mainly focused on more noticeable blackout events that usually resulted from cascading failures. From the aspect of outage and restoration times, substantially longer datasets were recently analyzed in Refs. [27,28]. The first study, composed of seven years of pan-European outage data, shows power-law fits with exponents of 1.7 and 2.1 for energy and power dimensions, respectively. The second study analyzes 14-year restoration time data of the Bonneville Power Administration, and a power-law fit (1.84) is shown to be the most suitable among other distributions, but empirical data have a slightly heavier tail than the fit.

In this paper, the collected data record all types of forced outage events due to individual component failures, be they almost negligible or affecting consumers from vast regions. The natural question is then if heavy tails could still emerge for accessible statistics, such as for the distributions of unavailable energy and unavailable duration [29]. And if so, what are the implications of these heavy tails? In what follows, we should be poised to answer these questions. We show by spectral analysis that the interevent times and the outage frequencies in the database exhibit a constant and a PL decaying component. The former, valid for short times, indicates random events excluding SOC, while the latter, valid for longer time scales, suggests an SOC mechanism, in which the optimization of repairing capacity plays the role of tuning to a critical point. Note that even a large constant can suppress a PL decay [30].

Based on the SOC, we propose a simple model, which can describe the outage-repair competition, taking into account branchinglike failure cascades, and which is capable of showing outage duration critical exponents close to the observations. This model has already been explored in the statistical physics of sandpiles and reaction-diffusion systems. Based on this model we try to propose possible mechanisms for mitigating outage duration exponents. However, the spectral analyses of the outage durations tend to suggest that the HOT mechanism, based on maintenance resource optimization, may be more favorable for describing the empirical outage duration data.

The remainder of the paper is organized as follows. Section II presents the methods and data used for the research. Results for the empirical data are detailed in Sec. III. Section IV presents a discussion and an explanation of the results.

## II. DATA AND METHODS

### A. Outage data description

We collected outage data from various online public sources of transmission system operators (TSOs). From these data, we exclusively consider outages caused by individual component failures, and no blackout events are considered. The interested outage events may be caused by any component failure before the power is transmitted to the customer end, be it a generator failure or any failure in the course of power transmission, the latter of which includes failures such as transmission line failures, circuit breaker failures, switch failures, transformer failures, etc. Hence, the collected data are categorized in accordance with their nature, as follows.

(i) Generator outages. This category includes the European Network of Transmission System Operators for Electricity (ENTSO-E) online data for the unavailability of production and generation units [31] for control areas (see the definitions of these terms in the Appendix), the California Independent System Operator (CAISO) generation outage data [32], the Hungarian Transmission System Operator (Magyar Villamosenergia-ipari Átviteli Rendszerirányító, MAVIR) data on generation outages [33], and the production outage data from the Italian Power Exchange (Gestore dei mercati energetici, GME) Inside Information Platform [34].

(ii) Transmission outages. As remarked above, many different types of transmission infrastructures can go wrong. For simplicity, we identify two types of transmission outages, i.e., transmission line outages, which include not only line failures but also failures in circuit breakers, switches, etc., and transformer outages. In this regard, the Bonneville Power Administration (BPA) data provide both transmission line outages and transformer outages [35], while the Alberta Electric System Operator (AESO) historical transmission outage data [36] recorded

a hybrid of transmission line outages and transformer outages. A special case comes from the ENTSO-E data for the unavailability of transmission grids between control areas [37]), which only record transmission line outages and transformer outages between pairs of control areas. The data indicate that the majority of outages were caused by transmission line failures though.

Most of these data sources do not provide dataset dumps but rather data access APIs. Hence, we have employed automatic data-scraping methods to assemble as much data as possible for further analyses. Note that automatic data collection methods are particularly useful for data sources that are limited by single-time query quota restrictions. For a detailed account of the data collection, see the descriptions in the respective references [32–37] and the raw data repository [38].

All the data are formatted in terms of many outage entries, with several columns that contain IDs of outage events, IDs of the plants, lines, transformers, starting time and the ending times, type of outages, the unavailable power (or the installed power and the available power), etc. In this paper, we focus only on the statistics of unexpected outages that TSOs usually do not have precautions for prevention, which are usually due to natural causes, such as storms and lightning strikes, or failures of generator components and transmission facilities. To this end, we filtered out entries for any planned outages for maintenance. This amounts to selecting entries labeled “Unplanned outage” (or “Forced outage”) for the ENTSO-E data, entries labeled with “FORCED” outage type for the CAISO data, entries labeled with “Auto” outage type for the BPA data, and entries labeled with “UNPLANNED” unavailability type for the Italy GME data, while the Hungary MAVIR data are already for unplanned outages. The AESO data do not contain such a field for filtering, and we simply selected entries designated with “Significant Outage.”

Previously, it has been shown that the sizes of blackouts and outages, measured by various quantities (energy, power, affected customers, etc.), follow power laws characterized by exponents ranging from about 1.3 to about 2.0 [19,39]. However, as remarked in the Introduction, although several possible explanations, for example, SOC for the direct current model [19], cascade failures in the second-order Kuramoto model for alternating currents [13,40], and power-law city sizes [41], have been proposed to understand the emergence of these power laws, a conclusive, full account for the origin of these power laws has not yet been reached in the literature. Because of the complexity of power-grid systems and their interaction with the environment, with our everyday life and production activities, and with the plant operation and maintenance staff, then natural events, population distributions, power-grid infrastructure failures, human societal behaviors, responses of the maintenance staff to outage events, and so on could all contribute to the heavy tails

of various measures to a certain extent. In a forthcoming study, we investigate the occurrences of PLs in the generator capacity sizes [42]. As for HOT, to the best of our knowledge, power spectra analysis has not been carried out before.

To further probe the possible origins of these power laws, we first reproduce similar power-law observations with the collected outage data, with outage sizes measured by the unavailable duration ( $T_u$ ) and the unavailable energy ( $E_u = T_u \times P_u$ , where  $P_u$  denotes unavailable power); see the Appendix for a full account of how these quantities are obtained from each raw dataset. As will be shown later, empirical unavailable duration distributions could also manifest power-law tails. Since many outage quantities can take the form  $T_u \times$  certain measure, we hence speculate that the understanding of the manifested power law for the unavailable duration constitutes a crucial ingredient for the understanding of general power-law behavior in outage distributions.

## B. Methods of outage data analysis

Suppose that the studied measure of outage sizes is denoted by  $x$ , representing  $E_u$  or  $T_u$ . One can assume that  $x$  is drawn from a *continuous* probability distribution  $\text{Prob}(x)$ . In particular, empirical data usually display a power-law tail starting from a certain minimum value  $x_{\min}$  [43,44]. One can further assume that the tail part of the distribution is drawn from a *continuous* power-law distribution with probability distribution function

$$p(x) = \frac{\tau - 1}{x_{\min}} \left( \frac{x}{x_{\min}} \right)^{-\tau} \quad (1)$$

and cumulative probability function (CDF)

$$P(x) = \int_x^{\infty} p(x') dx' = \left( \frac{x}{x_{\min}} \right)^{-\tau+1}. \quad (2)$$

In what follows, when concrete data are studied, we associate  $\tau_E$  and  $\tau_T$  with the distributions of  $E_u$  and  $T_u$ , respectively, for distinction.

For an outage dataset of  $N$  entries, assuming that the power law starts to hold from  $x_{\min}$  so that the remaining  $n$  entries whose  $x \geq x_{\min}$  fit into a power law, the exponent  $\tau$  can then be estimated by maximizing the logarithmic value of the likelihood

$$p(x|\tau) = \prod_{i=1}^n \frac{\tau - 1}{x_{\min}} \left( \frac{x_i}{x_{\min}} \right)^{-\tau} \quad \text{for all } x_i \geq x_{\min}, \quad (3)$$

giving rise to the estimated exponent [43]

$$\hat{\tau} = 1 + n \left[ \sum_{i=1}^n \ln \frac{x_i}{x_{\min}} \right]. \quad (4)$$

However, since  $x_{\min}$  is usually not known *a priori*, one can select any value  $x = X$  as  $x_{\min}$  and obtain an estimation  $\hat{\tau}(x_{\min} = X)$ . In order to find the optimal estimation  $\hat{x}_{\min}$ , we resort to minimizing the Kolmogorov-Smirnov statistic distance [43]

$$D(x_{\min}) = \max_{x \geq x_{\min}} |S(x) - P(x)| \quad (5)$$

that quantifies the distance between the empirical CDF  $S(x)$  of the data for observations  $x \geq x_{\min}$  and CDF (2) for the best power-law fit of the data [with  $\tau = \hat{\tau}$  estimated by Eq. (4)] in the region  $x \geq x_{\min}$ .

For the unavailable duration  $T_u$ , to explore the crossover from short-time behavior due to quick routine maintenance to power-law behavior in the much longer maintenance regime, we separate the events with respect to a temporal threshold and perform power-law fittings for  $T_u \leq 24$  h and  $T_u > 24$  h, respectively. The threshold was determined based on consultations with experts from the fields of power system maintenance and reliability of electric machinery. According to operational experience, forced outages rarely end in permanent failures, as they are caused by random events and the majority of such failures can be corrected in a range of hours. On the other hand, major faults typically require specialized equipment and/or personnel, which is available to a limited extent on site. Service level agreements for operation and maintenance typically consider repairs to be started within 24 h, but as the correction of these major faults usually requires mechanical work and possible disassembly of the equipment, registered outage times are exceeding 24 h.

## C. Methods of spectral data analysis

For major outage events, where large-scale blackout could occur, the entire outage duration distribution (and its power-law tail) may be accounted for by the inverse Weibull distribution ( $\alpha x^{-\beta-1} e^{-\lambda x^{-\beta}} \sim \alpha x^{-\beta-1}$  for  $x \gg 1$ ) due to the symmetry of failures and restorations [45]. However, it is also possible that the studied data may include many intermittently occurred random outage events; then, contrary to Ref. [46], the inverse Weibull distribution could not fit the data to the whole range.

To demonstrate that the studied outage data are indeed composed of random outage events, characterized by white noise signals, as well as correlated events potentially resulting from cascading outages, we perform power spectral analyses [14,15] on the time series  $S(t)$ , which, similar to the number of ‘‘topplings’’ in the sandpile model [7], is the number of outage events at time  $t$ , and on the time series  $I(t)$  for the  $t$ th interval between successive outage events. In addition, the duration  $D(t)$  for the  $t$ th outage event can also be regarded as a time series and should be analyzed. For  $S(t)$ , we have used the accessible time resolution, either 1 h or 1 min, as the time unit, while for

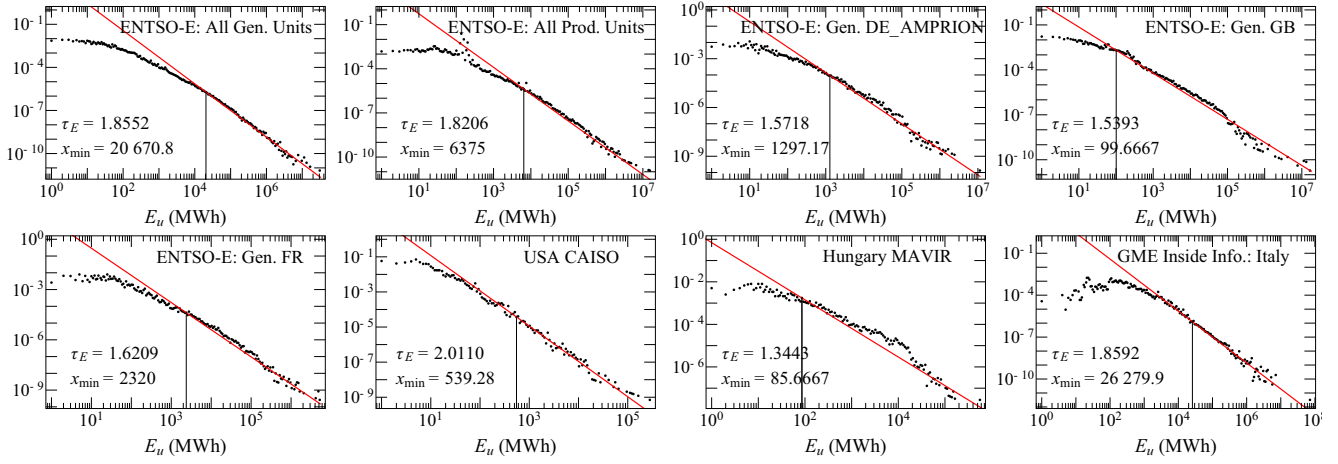


FIG. 1. Probability distributions (black dots) of generation outages measured in terms of the unavailable energy. For the ENTOSO-E data, we show the generation outage data for the control areas “DE\_AMPRION,” “GB,” and “FR,” as well as the generation and production outage data from all control areas. The fitted power laws and their corresponding  $x_{\min}$  values are marked by solid red lines and vertical black lines, respectively.

$I(t)$  and  $D(t)$ , the time  $t$  bears the meaning of the index of an event interval and the index of an event, respectively [47]. As an intuitive example for showing the effect of white noise on correlated signals, we also performed power spectral analyses on the noise signal  $N(t)$  obtained by superposing a Brownian noise with white noise of different intensities

$$N(t) = \sum_{i=1}^t X_i + Y, \quad t = 1, 2, \dots, T, \quad (6)$$

where  $X_i$  and  $Y$  are random variables drawn from the normal distributions  $\mathcal{N}(0, 1)$  and  $\mathcal{N}(0, \sigma)$ , respectively, with  $\sigma = 0, 1$ , and  $10$ . The power spectrum  $P_{\mathcal{F}}(f)$  of a signal  $\mathcal{F}(t) [= S(t), I(t), D(t), \text{ or } N(t)]$  is then computed as the absolute square of the discrete Fourier transform of  $\mathcal{F}(t)$  (via the fast Fourier transform) [48]:

$$H\left(f = \frac{t}{T}\right) = \frac{1}{\sqrt{T}} \sum_{k=1}^T \mathcal{F}(k) e^{2\pi i(k-1)(t-1)/T}, \quad (7)$$

$$P_{\mathcal{F}}(f) = |H(f)|^2 + |H(1-f)|^2, \quad 0 < f \leq \frac{1}{2}. \quad (8)$$

We remark that this analysis directly probes the correlation of raw outage events as well as their restorations; it is in contrast to probing the correlation of blackout events through their long-term correlations and the waiting times between successive blackouts [18].

### III. RESULTS

We categorize the outage statistics into outages in generation-production units and outages in transmissions

(see the Appendix for the difference between generation and production units). Note that transmission outages may be caused by various transmission infrastructure failures in transmission lines, transformers, circuit breakers, switches, etc.

#### A. Results on generator outages

Figures 1 and 2 show the probability distributions of outages in generation units and production units from various data sources as described in Sec. II A, measured in terms of unavailable energy and unavailable duration, respectively. In our analysis we considered both deratings of generation units and shutdowns; in the first case, the output capacity of the generator is lower than its nominal value, while in the latter case, we assume the complete loss of power output. In both cases, the volume of unavailable energy was determined by multiplying the duration of the outage with the power output considered to be unavailable. In real operating conditions, generator outages may present a wider spectrum, as presented in Refs. [49,50], where the authors also highlighted that, while generator outages are widely considered as individual events, significant correlations can be discovered between the outages.

For the ENTOSO-E data, we show results for all generation units and all production units, as well as results for several large control areas, including “DE\_AMPRION,” “GB,” and “FR” [30]. The distributions were obtained by binning the data logarithmically with base 1.08 first and then plotting on a log-log scale. These data distributions clearly display power-law tails. We employed the fitting method detailed in Sec. II B to determine  $x_{\min}$  and the power-law exponent  $\tau_E$  or  $\tau_T$ ; see also Table I in Sec. IV for a summary of the exponent values. For generation and production outages measured by the unavailable energy,  $\tau_E$

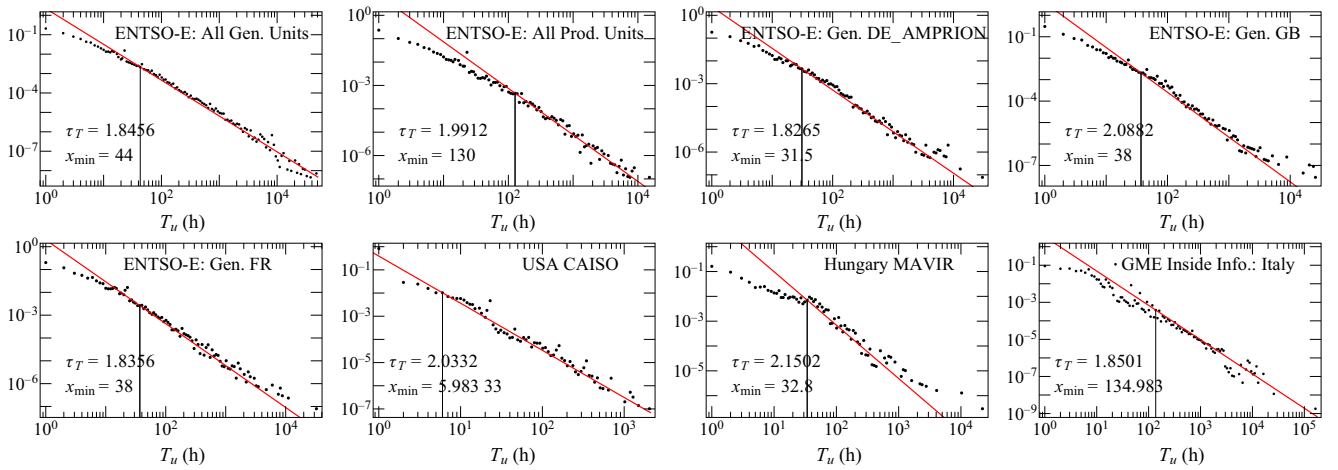


FIG. 2. Probability distributions (black dots) of generation outages measured in terms of the unavailable duration. For the ENTSO-E data, we show the generation outage data for the control areas “DE\_AMPRION,” “GB,” and “FR,” as well as the generation and production outage data from all control areas. The fitted power laws and their corresponding  $x_{\min}$  values are marked by solid red lines and vertical black lines, respectively.

ranges from about 1.3 to about 2.0, and for generation and production outages measured in terms of the unavailable duration,  $\tau_T$  ranges from about 1.8 to about 2.1. In addition to the statistics for generation and production units, Fig. 2 also shows the unavailable duration distributions for BPA customer services and BPA transformers, with  $\tau_T \simeq 1.83$  and  $\tau_T \simeq 1.09$ , respectively. Although here we only study single outage events, the observations for energy outage are thus comparable with the literature for blackout events [8, 19, 20, 22, 25, 27, 39]. What is more, the listed outage duration distributions further exemplify the findings for the transmission line restoration duration in Ref. [28] (there a power-law tail was identified with  $\tau_T \simeq 1.84$ ) and, here, for the restoration of outages in both generation and transmission facilities; see also the next subsection.

As remarked in Sec. II B, the 24-h threshold typically marks a separation for short- and long-time maintenance behaviors. One may then expect to observe quite

different statistics for  $T_u \leq 24$  h and for  $T_u > 24$  h. This is immediately justified by Fig. 3, upon applying the 24-h threshold on the duration of generation outages. Both the distributions for  $T_u \leq 24$  h and  $T_u > 24$  h display power-law tails (although distributions for the former case give weaker power laws with few orders of magnitude due to the threshold), hinting that maintenance activities are governed by different universal behaviors in short- and long-time maintenance.

## B. Results on transmission infrastructure outages

Unlike centralized power plants, transmission infrastructures are much more widely distributed over large regions. As such, in the way of power transmission, any failed transmission lines, switches, circuit breakers, transformers, etc., could cause outages. The BPA data provide both outage duration data for transmission lines (including

TABLE I. Summary of the various exponents obtained for energy outages ( $\tau_E$ ) and for outage duration ( $\tau_T$ ), with available  $\tau_T$  for  $T_u \leq 24$  h (denoted  $\tau_{T \leq 24}$ ) and  $T_u > 24$  h (denoted  $\tau_{T > 24}$ ) also displayed. The lower right part of the table shows results for transmission outage duration between pairs of control areas in the ENTSO-E data. Note that a similar set of exponents exists for pairs of control areas in a reversed transmission order (such as “ENTSO-E SE-NO”). The corresponding exponents are quite close to those shown in the lower right part of the table and are not included.

Generation	$\tau_E$	$\tau_T$	$\tau_{T \leq 24}$	$\tau_{T > 24}$	Transmission	$\tau_T$	$\tau_{T > 24}$
ENTSO-E all gen.	1.86	1.85	1.43	1.86	BPA transmission	1.85	1.72
ENTSO-E all prod.	1.82	1.99	1.34	2.24	BPA transformer	1.09	1.17
ENTSO-E DE_AMPRION	1.57	1.83	1.40	1.90	AESO	2.37	2.37
ENTSO-E GB	1.54	2.09	1.49	2.02	ENTSO-E all transmission	1.54	1.54
ENTSO-E FR	1.62	1.84	1.50	1.84	ENTSO-E DE_50HZ-PL_CZ	1.07	1.01
USA CAISO	2.01	2.03	1.47	2.20	ENTSO-E NO-SE	1.12	1.12
Hungary MAVIR	1.34	2.15	1.08	2.14	ENTSO-E PT-ES	1.25	1.25
GME Italy	1.86	1.85	1.54	1.85	ENTSO-E SE-DK_CA	1.00	0.97

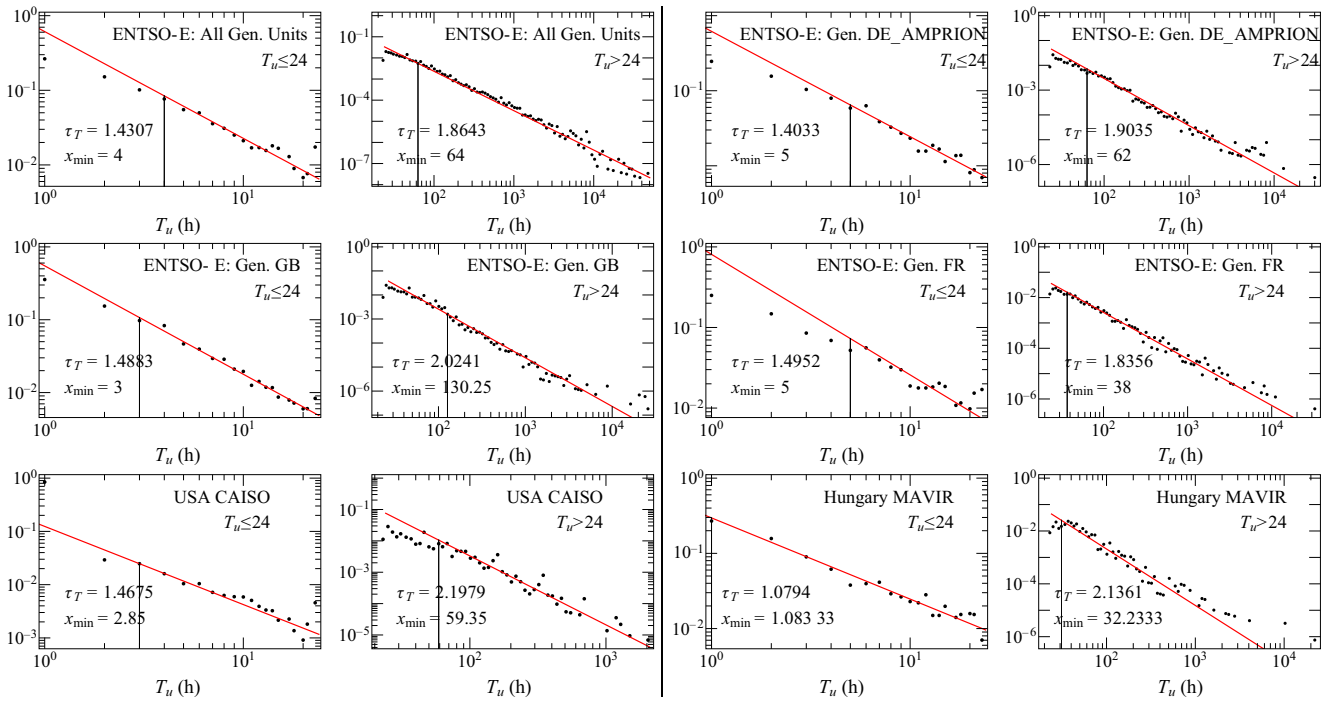


FIG. 3. Probability distributions (black dots) of generation outages measured in terms of the unavailable duration, with the duration separated by a threshold at 24 h. The fitted power laws and their corresponding  $x_{\min}$  values are marked by solid red lines and vertical black lines, respectively.

switch and circuit breaker failures) and outage duration data for transformers separately; the data are shown in the two top panels of Fig. 4. In these two cases, as in Ref. [28], the power-law tails are quite evident, and the smaller exponent for transformer outages, in accordance with our intuition, suggests that restoring the functionality of a transformer is more likely to take a longer time as compared to repairing a transmission line. Power-law tails manifest even if the data contain a mixture of outage events caused by both transmission line failures and transformer failures, as shown by the two bottom panels of Fig. 4 for the AESO data and the combined ENTSO-E data for transmission outages between all pairs of control areas (see below for a few examples on some selected control area pairs).

Hence, not only transmission line failures and transformer failures but also their mixture could lead to power-law outage distributions. The latter can be made sensible via a mixture distribution [51]. For a data source with  $x$  drawn from several distributions  $p_1(x), p_2(x), \dots, p_n(x)$  and weights  $w_1, w_2, \dots, w_n$ , where  $w_i > 0$  and  $\sum_i w_i = 1$ , the mixture distribution for  $x$  would be  $p_m(x) = \sum_i w_i p_i(x)$ . Let us assume that general transmission outage events can be caused by both transmission line failures and transformer failures, which follow the power-law distributions  $p_1(x) = k_1 x^{-\tau_{T1}}$  and  $p_2(x) = k_2 x^{-\tau_{T2}}$ , respectively, in the tails. Now if the events happen with weights  $w_1$  and  $w_2$ , the tail part  $[x > (k_1/(\tau_{T1} - 1))^{1/(\tau_{T1}-1)}$  and

$x > (k_2/(\tau_{T2} - 1))^{1/(\tau_{T2}-1)}$ ] of the mixture distribution will be given by

$$p_m(x) = \frac{1}{w_1 + w_2} (w_1 k_1 x^{-\tau_{T1}} + w_2 k_2 x^{-\tau_{T2}}) \sim x^{-\tau_T}, \quad (9)$$

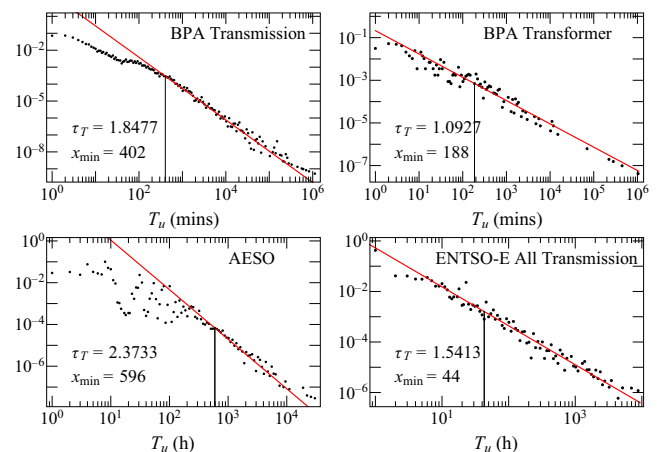


FIG. 4. Probability distributions (black dots) of various types of transmission outages measured in terms of the unavailable duration. The fitted power laws and their corresponding  $x_{\min}$  values are marked by solid red lines and vertical black lines, respectively.

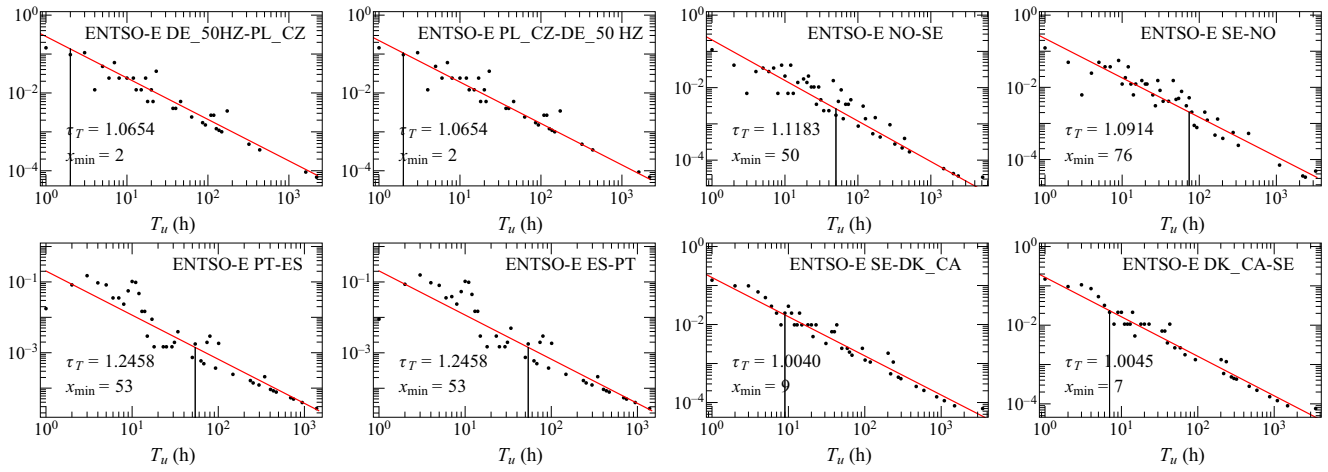


FIG. 5. Probability distributions (black dots) of transmission outages between pairs of control areas (labeled at the top of each panel), measured in terms of the unavailable duration. The fitted power laws and their corresponding  $x_{\min}$  values are marked by solid red lines and vertical black lines, respectively.

so that the tail is dominated by the power law of the smaller exponent  $\tau_T = \min(\tau_{T1}, \tau_{T2})$ , as long as  $w_1 \sim w_2$ .

The above argument can now be readily extended to understand the observed power law of the ENTSO-E transmission outage duration for all pairs of control areas, given each pair of them follows a power law. To check this, in Fig. 5 we show transmission outage duration distributions for a few pairs of control areas. Since the sizes of most such datasets are too small to give good enough statistics, the displayed data are specifically selected for pairs of larger control areas that contain enough outage events. From the figure, we see that, for these larger control areas, the transmission outages between them indeed follow power laws in outage duration distributions and typically have an

exponent  $\tau_T$  ranging from about 1.0 to about 1.3, suggesting that transmission infrastructures between larger control areas are more difficult to fix if they fail. Since the exponents in these examples are fairly small, then according to Eq. (9), it is tempting to conjecture that the overall exponent will be  $\tau_T \sim 1$  if we combine the data for all pairs of control areas. However, out of 226 datasets for different pairs of control areas, only a few are large enough to show meaningful statistics, so their weights are almost negligible. Hence, the exponent  $\tau_T \sim 1.54$  from Fig. 5 must be ascribed to the overall statistics of smaller control areas and, theoretically, they should be governed by larger exponent values, even though the dataset of each of them is yet too small to show significant statistics.

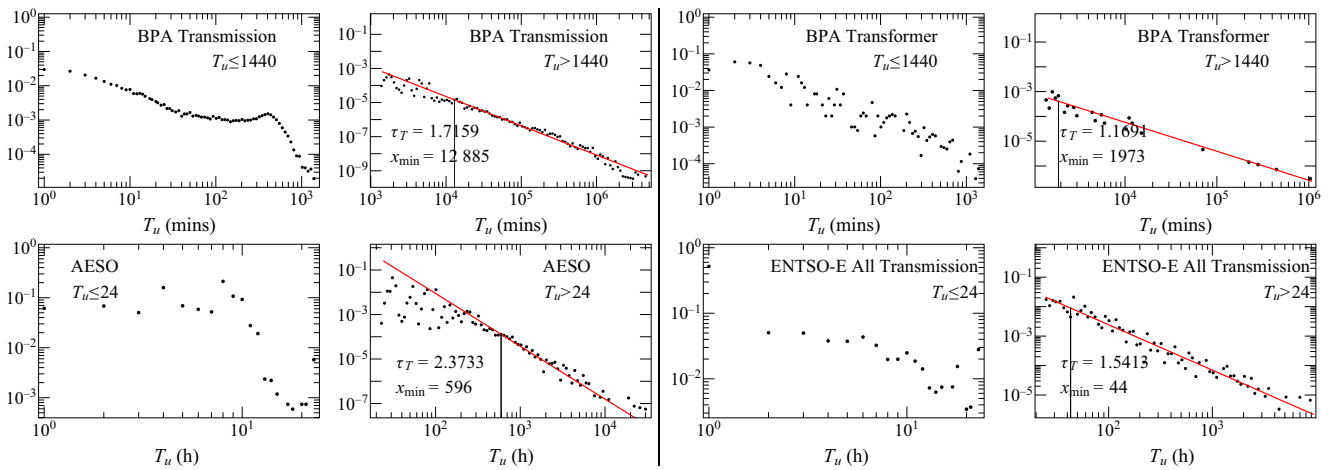


FIG. 6. Probability distributions (black dots) of transmission outages measured in terms of the unavailable duration, with the duration separated by a threshold at 24 h (1440 min). For  $T_u > 24$  h, the fitted power laws and their corresponding  $x_{\min}$  values are marked by solid red lines and vertical black lines, respectively. For  $T_u \leq 24$ , unlike in Fig. 3, the statistics are not justifiable for power-law fits.



In Figs. 6 and 7, a 24-h threshold is again applied to the duration of transmission outages corresponding to Figs. 4 and 5, respectively. In contrast to generation outages in which 24 h separates two different universal behaviors due to maintenance teams' responses in a specific power system, transmission outage duration only shows power-law tails for  $T_u > 24$ , while for  $T_u \leq 24$  h, power-law tails are hardly observed due to either a genuine lack of power laws or probably too small sample sizes. If the former is the case, it may be that transmission lines usually locate in remote places, many of which could only be fixed with a longer time so that only longer-time maintenance activities follow a universal behavior.

#### IV. DISCUSSION

We summarize the obtained exponents in Table I. As mentioned earlier, the exponent  $\tau_E$  for the unavailable energy shows good agreement with the literature. For outage duration in the generation sector, we conclude that a 24-h threshold typically renders  $\tau_{T \leq 24} \sim 1.0\text{--}1.5$  and  $\tau_{T > 24} \sim 1.80\text{--}2.20 \sim \tau_T > \tau_{T \leq 24}$ . For transmission infrastructure outage duration, even though the statistics are not good enough for power-law fits when  $T_u \leq 24$ , we still see that  $\tau_{T > 24} \sim \tau_T$ . Hence, the observed power-law tail for  $T_u$  for each dataset is essentially unaffected if outage events with  $T_u \leq 24$  are all excluded. These results suggest that typical outages not yet restored beyond 24 h are governed by a universal mechanism that gives rise to heavy tails.

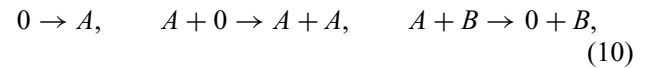
##### A. Potential explanations for heavy tails

Since many outage measures are related to the duration of the outage events, these observations for unavailable duration distributions thus provide another perspective to understand the ubiquitous existence of heavy tails in power-grid systems. In the following, potential explanations of the underlying phenomena are presented. The explanations are structured as follows: (i) the potential relation to SOC, (ii) the potential relation to HOT, and (iii) a summary arguing for more analysis and the need for more detailed empirical data.

(i) Empirical data of faulty electrical (and many other types of) components may show exponential distributions [52], but, in general, have been described by lognormal, gamma, or Weibull repair time distributions [53]. Furthermore, the heavy-tailed outage durations we observe in the databases may be the consequence of dependent events. In Sec. IV B we provide a power-spectral analysis, which shows power-law decaying autocorrelations for quite a proportion of the outage events. A possible explanation for the correlations among the repairs can be related to the limited capacity or availability of the maintenance staff or equipment within a region. Thus, the observed power laws can have a similar origin as those of the cascading blackout events themselves: SOC [7,54], tuned by

the competition of supply and demand, to the edge of a critical point [19,39], which is optimal for the function of the whole economy [55]. In other words, keeping too large a maintenance capacity is economically inefficient, while too small is dangerous for the function of the whole power grid; therefore, the maintenance staff and resources of the system tune them to a SOC state as in the case of power production. One can naturally view the heavy tails in outage duration distributions as a direct result of the responses of maintenance resources to outages of different scales driven by SOC.

To understand the critical exponents and how crossover behavior can emerge, one can map the outage process onto simple nonequilibrium reaction-diffusion (RD) models with phase transitions. Such mappings have been shown to be very efficient at describing universal behaviors of nonequilibrium systems [56]. Let us quantify outage sizes in terms of the time integral of failed units until repair. SOC appears when a slow drive (particle adding in RD models) and a faster dissipation (particle removal in RD models) mechanism compete [57,58]. Denoting functioning units by 0 "particles," faulty (active) ones by  $A$ 's, and the repairing teams by  $B$ 's, we can set up the reaction scheme



where the number of  $B$ 's can be considered a conserved quantity. They move in the system and their role is only to sustain the system's function. The  $0 \rightarrow A$  describes the slow drive, while the  $A + 0 \rightarrow A + A$  models the fast redistribution ending with the dissipative  $A + B \rightarrow 0 + B$  repair process, in agreement with a SOC model. The outage size is then measured by the time integral of the number of  $A$ 's in a SOC avalanche. This simple system can be considered as the combination of spontaneous isotropic percolation [59] (IP) and a branching process, describing a possible failure cascade, which implies the criticality of the directed percolation [60], coupled with a conserved density (DP-C) [56], as  $B$  can be regarded as a background and the total number  $N_A + N_0$  is conserved [61]. The process takes place on a network of interacting electrical units that may contain long-range interactions. The interacting network can be quite different from the physical connection network, which is presumably small-world like, and for high-voltage nodes, we showed [13,40] that power grids have graph dimensions between 2 and 3, but we do not know the network of the components of the database. For example, it has been shown in Ref. [62] that cascading transmission line outages can be described by Markov chain transition matrices, with which non-local interactions of transmission lines can be observed. When there is no particle number conservation in the system, we know that, for regular networks, the DP critical

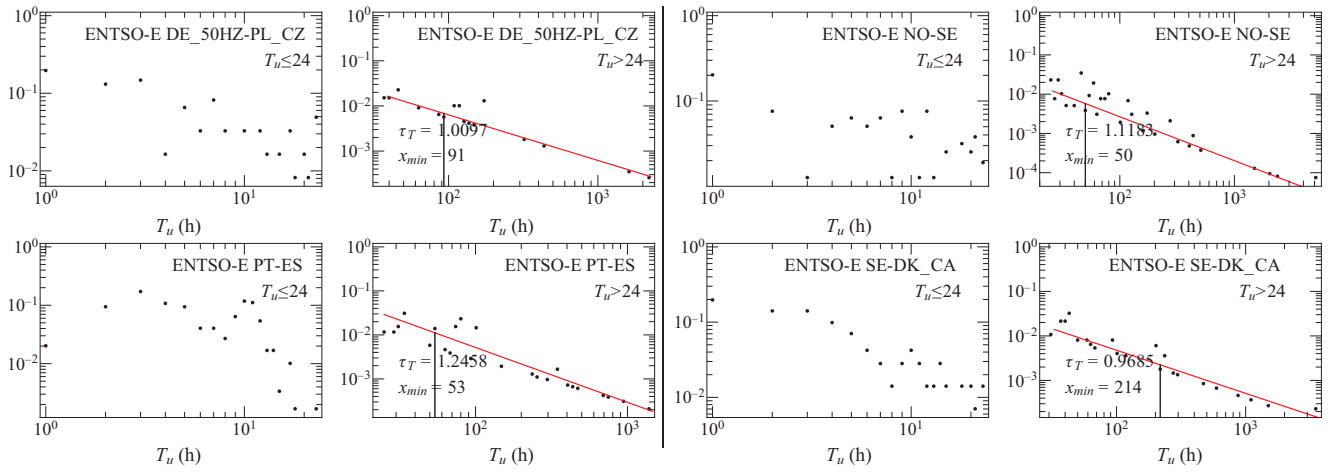


FIG. 7. Probability distributions (black dots) of transmission outages measured in terms of the unavailable duration, with the duration separated by a threshold at 24 h (1440 min). For  $T_u > 24$  h, the fitted power laws and their corresponding  $x_{\min}$  values are marked by solid red lines and vertical black lines, respectively. For  $T_u \leq 24$ , unlike in Fig. 3, the statistics are not justifiable for power-law fits.

fixed point is stable asymptotically as compared to the IP [63,64], so a crossover may happen between IP to DP. Such crossover between critical points has also been studied in the IP + DP model in the case of brain models [65], on different complex networks. Then, similarly, with the conserved reactions (10), we should expect an IP to DP-C crossover. If the spontaneous failure probability is small, it does not cause a critical DP-C percolation, but a slightly off-critical one, which cannot be distinguished from wandering around DP-C criticality as in the case of SOC-like models [66].

In the case of this DP-C SOC process, we can expect the occurrence of avalanches, triggered by failures of single units, with a power-law size distribution. As for the outage duration distribution, the outage times of single units can be related to the autocorrelation function, which gives the probability of an outage  $A$  still not yet being restored after  $T_u$ , and which exhibits the asymptotic scaling:  $C_{AA}(T_u) \propto T_u^{-\lambda/Z}$ , where  $\lambda$  is the autocorrelation exponent and  $Z$  is the dynamical exponent of the critical process [56]. Put another way, this probability can also be expressed in terms of the outage duration distribution  $P_T(T_u)$  as

$$\int_{T_u}^{\infty} P_T(T) dT = C_{AA}(T_u), \quad (11)$$

giving rise to  $P_T(T_u) \sim T_u^{-\tau_T} = T_u^{-\lambda/Z-1}$ .

Since the inert 0s are intrinsically not moving, the scaling properties of reactions (10) then belong to the so-called Manna universality class [56,67], which also encompasses the conserved threshold transfer process in  $d \geq 2$  dimensions [56,67,68]. By utilizing the scaling relation  $\lambda = d - \Theta$  [56,69], where  $\Theta$  is the initial slipping exponent, we

obtain

$$\tau_T = d/Z - \Theta + 1. \quad (12)$$

Inserting the numerical values for  $\Theta$  and  $Z$  from Ref. [56,67] gives  $\tau_T \approx 1.37, 1.99$ , and  $2.51$  in 1, 2, and 3 dimensions. The exponent value in 2 dimensions seems to agree with our database analysis for generation outages that resulted in  $1.8 \leq \tau_T \leq 2.1$ , depending on the region of the data. The exponent values for transmission outages span a wider range, but still seem to be close to the model values in 1 to 3 dimensions. These exponents suggest a fairly universal asymptotic behavior. Differences from the theoretical values can be the consequence of SOC quasicritical behavior by the spontaneous failures, under-sampling, different networks with different dimensions, or even Griffiths effects [70,71], which occur in the case of quasistatic heterogeneity of the system.

We do not have data for the failure cluster size distributions, but for the distribution of lost energy  $E_u$ , which is related to the product of the outage duration  $T_u$  and the unavailable power capacity  $P_u$  of the nodes, which also shows power-law distributions for certain databases (for example, in the CAISO data); the power-law tails of  $E_u$  follow immediately from that of  $T_u$ .

(ii) The above-simplified model unavoidably leaves out many complications. First, as outages do not necessarily occur in a SOC cascading manner, the heavy tails in outage duration distributions may not be fully accounted for by the responses of the limited maintenance resources to the SOC cascading failures, as we assumed above. Second, the *ad hoc*  $B$  agents themselves, albeit being considered conserved for simplicity, should be organized as a result of further hidden mechanisms for achieving economically

efficient responses to outages, so they are not strictly conserved in a long-time span. What is more, the above simple model only regards  $B$ 's as a background, so that their spatial distribution as well as how they will move in response to the generations of  $A$ 's are totally discarded, whereas, in reality, some generators in the network may be considered more crucial than others or have to provide higher availability or meet contractual maximum outage criteria. Operators keep extra resources for such facilities to recover more quickly from outage types that would normally cause a longer outage time, thus skewing the outage time distribution towards smaller outage times.

Since man-made complex systems like power-grid systems are highly structured and dominated by optimization designs, the above considerations point to another mechanism for the observed heavy tails: the HOT mechanism [9,72]. For forest fires and sandpiles as exemplified in Ref. [9], the HOT mechanism introduces barriers (the resources) to minimize the expected size of the event. These barriers are concentrated in the regions that are expected to be most vulnerable, leaving open the possibility of large events in less probable zones. So in this way, power-law size distribution can emerge by minimizing the average event size via the variational principle with respect to the resource distribution function, subject to the restriction of resources used to construct the Lagrange multiplier. Hence, even for outage events, although the SOC mechanism can play a role regionally, we cannot exclude that, in the pursuit of optimization in the maintenance resource distribution and minimization of outage times, the HOT mechanism could partially contribute to the heavy tails in outage size distributions globally.

To be more specific, consider that *independent* cascading outage events, be they uncorrelated single outage events or blackout events, can be indexed by  $1 \leq i \leq N$ . In the original HOT mechanism, the resources  $r_i$  are allocated to suppress an event of size  $l_i$  from happening, obeying a map  $l_i = F(r_i)$ . By minimizing the expected outage size [72]

$$J = \left\{ \sum p_i l_i | l_i = F(r_i), \sum r_i \leq R \right\}, \quad (13)$$

subject to the limited resource  $R$ , it was shown that the size distribution follows a power law  $P(l) \sim l^{-\alpha}$ . In the above expression,  $p_i$  denotes the probability of event  $i$  during some time span of observation. The general idea is of course to allocate the resources to places where a large-size event is more likely to happen. However, in the context of outage duration, the focus becomes utilizing the limited resources  $R$ , say the available maintenance manpower in hours, to fix outages lasting for various times  $T_u$  during the observation time span. Now an event should be directly considered as an outage caused by a generator failure or a transmission infrastructure failure. These events of course do not necessarily occur independently, but for a long

enough time span, each of these outage events, indexed by the location  $i$  for instance, should associate with a probability  $p_i$  and an expected restoration time (outage duration)  $T_{ui}$ . In this sense, the outage events are again considered as *independent*, and by extending the HOT mechanism (13), the observed heavy tails in outage duration distributions may be attained by minimizing the objective cost

$$J = \left\{ \sum p_i T_{ui} | T_{ui} = g(r_i), \sum r_i \leq R \right\}. \quad (14)$$

For the above purpose, the maintenance manpower is naturally concentrated in regions where outages happen more frequently, leaving an outage event in a remote place needing a longer time to fix, even if it is just a trivial one. Hence, heavy tails  $P_T(T_u) \sim T_u^{-\tau T}$  ensue in outage duration distributions in a similar manner as the original HOT mechanism for outage sizes. Nevertheless, at this stage, the HOT explanation can only be a hypothesis as we still lack knowledge of  $p_i$  and the functional form of  $g(r)$ . What is more, while it is critical to know the dimension of the grid for HOT predictions for cascading sizes, for a more general quantity like the outage duration  $T_u$ ,  $g(r)$  is determined by the resource-loss relationship, which may or may not be directly related to the physical dimension [72].

(iii) Our empirical results show similarities with experiences of the power sector as well. Vinogradov *et al.* [73] concluded, based on the data of a regional power supply company, that the most frequent causes for transmission outages are shortcomings in maintenance, natural and weather conditions, and unauthorized personnel. It is also known that preventive maintenance highly affects the availability of the equipment, but it comes at a cost (monetary and human resources) [74,75].

By considering all these intertwined factors, we see that there are various aspects for the emerged heavy tails in outage statistics. On the one hand, some intervention measures, which are usually not optimized, are introduced to the infrastructure, so that outage events do not entirely occur in a spontaneous SOC manner, but SOC processes could still dominate in many parts of the system. On the other hand, in response to outage events, maintenance resources enjoy bigger flexibility and may be optimally deployed as needed. In summary, our above discussion favored a SOC explanation for the occurrences of outage events, but we do not entirely exclude the HOT mechanism, whereas, for outage duration, it is more plausible to ascribe the observed heavy tails to an extended HOT mechanism. For outages, since the HOT mechanism restricts more probable large-size events from happening, it is suggested that the  $1/f$  spectra may not be observed, contrary to SOC processes [12]. To partially unravel if it is a SOC or HOT mechanism in play for outage events and their duration, in the next section, we try to detect if there are any

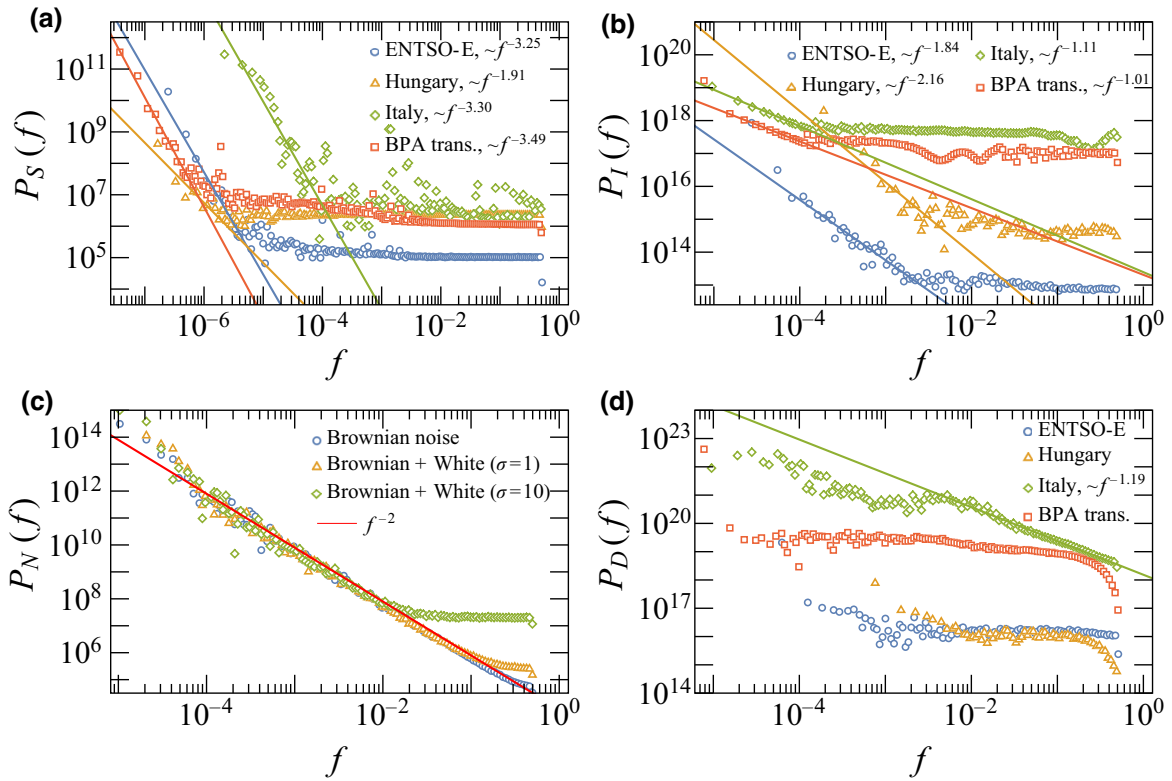


FIG. 8. Power spectra of the time series of (a) the number of outage events  $S(t)$ , (b) the intervals between successive outage events  $I(t)$ , (c) the Brownian noise  $N(t)$ , with and without the presence of a white noise background, and (d) the outage duration  $D(t)$ . In panels (a), (b), and (d), we show the respective power spectra for the ENTSO-E generation outage data from all control areas, the Hungarian MAVIR generation outage data, the GME Italian generation outage data, and the BPA transmission outage data.

traits of  $1/f$  noise by performing power spectral analyses on outage and restoration time series.

### B. Power spectral analysis

In this section, we employ the spectral analysis method on the time series  $S(t)$ ,  $I(t)$ ,  $D(t)$ , and additionally  $N(t)$ , all introduced in Sec. II C. As shown in Figs. 8(a) and 8(b), our collected outage data typically display a  $1/f^\alpha$  power law, a signature of correlation in the outage events, in the lower-frequency range, while the higher-frequency range is overwhelmed by white noise, which is characterized by a constant power spectrum. This is immediately evident if we compare Figs. 8(a) and 8(b) to how the  $1/f^2$  power spectrum of a Brownian noise is affected by white noise of different intensities, as illustrated in Fig. 8(c). Hence, even though the exponent values for  $P_S(f)$ , ranging from about 1.91 to about 3.49, are not entirely in accord with  $\alpha < 2$  for the Bak-Tang-Wiesenfeld and Manna sandpile models with dimensionality  $d < d_c = 4$  [76], we do not exclude that the topology of the system may come into play, or that there could exist a crossover in the  $1/f^\alpha$  law, as the correlations manifested in the higher-frequency range are largely masked by white noise.

Since the majority of the outage events seem to occur out of quite random causes, the above observations suggest that the manifested power laws in outage duration distributions cannot be attributed to the responses to cascade blackout events alone. In Fig. 8(d), we show that the outage duration time series  $D(t)$  barely shows any evident traits of  $1/f$  noises, except for the Italy data, in which the events were recorded hourly instead of every minute. Since many outage events can be fixed in a matter of a few hours, we suspect that the  $1/f$  noise in the high-frequency part (short time) of the Italy data merely reflects a superficial correlation of outage duration due to its low temporal resolution. Based on these arguments, the pervasive heavy tails in outage duration distributions may then be more deeply rooted in the modified HOT mechanism conjectured in Ref. (14), featuring the optimized responses of the limited maintenance resources to both random outage events as well as cascade outage events resulting from SOC processes.

For outage events, the observed  $1/f$  noises strengthen the complex IP + DP-C SOC hypothesis advanced before, calling for a dominating branching process for long times and a branching process overwhelmed by random events for short times and excluding the HOT explanation for outage sizes. Yet, the vastness of those random, singular events may be partially a result of the

aforementioned barriers introduced to strengthen the power grids, which prevent failures from spreading further. For the  $\alpha < 2$  interevent cases, nonergodicity, aging, and consequently an age-dependent scaling can also occur [77], related to so-called “crucial events.”

## V. CONCLUSIONS

In the present paper, we revisited the topic of the size distribution of forced outages in power systems to formulate possible theoretical explanations of the uniformness of these distributions. To address a shortcoming of previous studies, long-term outage data of various power systems were collected and analyzed. First, exponents of power-law fits were extracted to cross-check the results with related literature; then this step was repeated after setting a threshold, speculating that the understanding of the manifested power law for the unavailable duration constitutes a crucial ingredient for the understanding of general power-law behavior in outage distributions. Based on the numerical results, potential explanations were presented, and a power spectral analysis was performed to demonstrate that the studied outage data are composed of many random events as well as some correlated events characterized by the  $1/f$  noise. This hints that SOC processes could take place in outage events. Therefore, for outage events, we consider the system under study as the combination of spontaneous isotropic percolation and a branching process, implying DP-C criticality. Although a SOC explanation based on the DP-C criticality for the heavy tails in outage duration distributions is tempting, given that the majority of the outage events occurred out of random causes, the manifested power laws in outage duration cannot be attributed to the responses to SOC cascading failures alone. The power spectra of the outage duration time series further indicate a lack of  $1/f$  noise, leading us to conjecture an extended HOT explanation for the heavy tails in outage duration distributions. This can be quite sensible, as on the one hand, power-grid infrastructures are built more or less in a self-organized manner to meet customers’ demands, so they are more rigid to give rise to SOC processes, despite some measures being introduced to confine the spread of outages; on the other hand, the needed maintenance resources in responses to outage events can be more fluidly distributed and allocated, permitting a greater extent of optimization for economical efficiency.

Since cascading failures pose higher risks to society, the statistical physics approach to critical phenomena opens up the possibility to provide suggestions on how to make cascade-failure-like outages smaller. In general, the addition of long-range interactions, suppresses fluctuations and increases the effective graph dimensions, making the processes more mean field like, which are faster, with shorter outage durations corresponding to larger  $\tau_T$  [56]. On the other hand, quenched heterogeneity and modular structures

slow down the critical dynamics. This can be seen in our analysis where we found smaller outage exponents for transmissions between control areas than within them. Thus, increasing the size or decreasing the number of control areas should decrease the outage times. It is also known in statistical physics of critical systems that in multicomponent models, spatial anisotropy can alter the universal scaling behavior [56]. In particular, for the DP-C class sandpile models, spatial anisotropy or an absorbing wall increases the  $\tau_T$  critical exponent [78], which could be exploited by deploying efficient service team geometry or topology.

In the future, it would be interesting and valuable to examine in depth more structured data that allows a proper separation of cascading events and random outages so that one can compare how these two types of events are restored differently. If such information cannot be directly inferred from the raw data, one approach is to group outages into cascades and generations within each cascade according to their relative occurrence timing [79]. In a more recent work [16], transmission system outage data were also structured into resilience events (onset and full restoration of cascading outages) according to the timing of outages and restorations, with which several metrics were proposed to evaluate the duration of these resilience events. As power-grid systems consist of many coupled subsystems and are constantly subjected to various kinds of drive and dissipation, understanding the pervasive heavy tails in various measures is always challenging. To gain a better understanding, it will also be interesting to set up simple hybrid models with the SOC mechanism, similar to the OPA model [26], to account for the outage events and the HOT mechanism for optimizing the restoration processes.

## ACKNOWLEDGMENTS

Support from the Hungarian National Research, Development and Innovation Office NKFIH (K128989) and from the ELKH grant SA-44/2021 is acknowledged.

## APPENDIX: QUANTITIES EXTRACTED FROM THE RAW DATASETS

The quantities of interest are the outage duration  $T_u$  and the unavailable power  $P_u$ . They are extracted from the raw datasets [38] as follows.

(i) Generator outage data.

(a) The ENTSO-E data for different control areas in Europe [31]. The relevant columns of each entry are those named “avail\_qty” (available power, in megawatts), “end” (outage ending time), “nominal\_power” (installed power, in megawatts), and “start” (outage starting time). Hence,  $P_u = \text{nominal\_power} - \text{avail\_qty}$  and  $T_u = \text{end} - \text{start}$  (in hours). Here we also give the definitions for

a few terminologies. According to the ENTSO-E data descriptions, a generation unit is “a single electricity generator belonging to a production unit,” while a production unit is understood as “a facility for generation of electricity made up of a single generation unit or of an aggregation of generation units.” According to the document “Commission Regulation (EU) No 543/2013 of 14 June 2013 on submission and publication of data in electricity markets,” a control area “means a coherent part of the interconnected system, operated by a single system operator and shall include connected physical load and/or generation units if any.”

(b) The CAISO data for California [32]. We use prior trade date reports with fields for both the unavailable duration and unavailable power included. The relevant columns are those named “CURTAILMENT START DATE TIME,” “CURTAILMENT END DATE TIME,” and “CURTAILMENT MW”:  $T_u = \text{“CURTAILMENT END DATE TIME”} - \text{“CURTAILMENT START DATE TIME”}$  (in hours),  $P_u = \text{“CURTAILMENT MW”}$ .

(c) The MAVIR data for Hungary [33]. The relevant columns are those named “Start of the outage,” “End of the outage,” and “Unavailable capacity” (in megawatts):  $T_u = \text{“End of the outage”} - \text{“Start of the outage”}$  (in hours),  $P_u = \text{“Unavailable capacity”}$ .

(d) The GME data for Italy [34]. The relevant columns are those named “EventStart,” “EventStop,” and “UnavailableCapacity”:  $T_u = \text{EventStop} - \text{EventStart}$  (in hours) and  $P_u = \text{UnavailableCapacity}$  (in megawatts).

(ii) Transmission infrastructure outages.

(a) The BPA data for the Pacific Northwest of the United States [35]. This dataset monitored customer service interruptions, transmission line interruptions, and transformer interruptions. For the purpose of this paper, only the data for transmission line interruptions and transformer interruptions were selected, while the data for customer service interruptions were not considered because they contain blackouts for customers in different districts, which are usually consequences of multiple outage events and last as long as any infrastructure failures in a district are not restored. For the selected datasets, the relevant column is  $T_u = \text{“Duration”}$  in minutes.

(b) The AESO historical data for Canada [36]. The relevant columns are “Outage Start” and “Planned End,” giving  $T_u = \text{“Planned End”} - \text{“Outage Start”}$  in hours.

(c) The ENTSO-E data for transmission outages between pairs of control areas in Europe [37]. There are 65 control areas in total [38], out of which, only 226 ordered pairs of control areas have direct power exchanges. Similar to the ENTSO-E generator outage data, the relevant columns of each entry are those named “avail\_qty” (available power, in megawatts), “end” (outage ending time), “nominal\_power” (installed power, in megawatts), and “start” (outage starting time).

Hence,  $P_u = \text{nominal\_power} - \text{avail\_qty}$  and  $T_u = \text{end} - \text{start}$  (in hours). In the main text, we only show the analysis for  $T_u$  in parallel with the analyses for the BPA and the AESO data.

- 
- [1] W. K. Härdle and B. L. Cabrera, Calibrating CAT bonds for Mexican earthquakes, *J. Risk. Insur.* **77**, 625 (2010).
  - [2] A. Chernobai, K. Burnecki, S. Rachev, S. Trück, and R. Weron, Modelling catastrophe claims with left-truncated severity distributions, *Comput. Stat.* **21**, 537 (2006).
  - [3] A. Chatterjee and B. K. Chakrabarti, Fat tailed distributions for deaths in conflicts and disasters, *Rep. Adv. Phys. Sci.* **01**, 1740007 (2017).
  - [4] N. N. Taleb, *The Black Swan* (Random House, New York, NY, 2007).
  - [5] G. De Marzo, A. Gabrielli, A. Zaccaria, and L. Pietronero, Quantifying the unexpected: A scientific approach to black swans, *Phys. Rev. Res.* **4**, 033079 (2022).
  - [6] A. Abedi, L. Gaudard, and F. Romero, Review of major approaches to analyze vulnerability in power system, *Reliab. Eng. Syst. Saf.* **183**, 153 (2019).
  - [7] P. Bak, C. Tang, and K. Wiesenfeld, Self-Organized Criticality: An Explanation of the  $1/f$  Noise, *Phys. Rev. Lett.* **59**, 381 (1987).
  - [8] B. Carreras, D. Newman, I. Dobson, and A. Poole, Evidence for self-organized criticality in a time series of electric power system blackouts, *IEEE Trans. Circuits Syst. I Regul. Pap.* **51**, 1733 (2004).
  - [9] J. M. Carlson and J. Doyle, Highly optimized tolerance: A mechanism for power laws in designed systems, *Phys. Rev. E* **60**, 1412 (1999).
  - [10] M. Stubna and J. Fowler, An application of the highly optimized tolerance model to electrical blackouts, *Int. J. Bifurcation Chaos* **13**, 237 (2003).
  - [11] X. Lin and Z. Bo, in *2008 IEEE Power and Energy Society General Meeting - Conversion and Delivery of Electrical Energy in the 21st Century* (IEEE, Pittsburgh, PA, USA, 2008), p. 1.
  - [12] G. T. Hohensee, Power law behavior in designed and natural complex systems: Self-organized criticality versus highly optimized tolerance, A Literature Review for Emergent States of Matter, Fall 2011 University of Illinois at Urbana-Champaign (2011).
  - [13] G. Ódor, S. Deng, B. Hartmann, and J. Kelling, Synchronization dynamics on power grids in Europe and the United States, *Phys. Rev. E* **106**, 034311 (2022).
  - [14] H. J. Jensen, K. Christensen, and H. C. Fogedby,  $1/f$  noise, distribution of lifetimes, and a pile of sand, *Phys. Rev. B* **40**, 7425 (1989).
  - [15] J. Kertész and L. Kiss, The noise spectrum in the model of self-organised criticality, *J. Phys. A: Math. Gen.* **23**, L433 (1990).
  - [16] I. Dobson and S. Ekisheva, How long is a resilience event in a transmission system? Metrics and models driven by utility data, arXiv preprint [arXiv:2208.06985](https://arxiv.org/abs/2208.06985) (2022).
  - [17] P. Hines, J. Apt, and S. Talukdar, Large blackouts in North America: Historical trends and policy implications, *Energy Policy* **37**, 5249 (2009).

- [18] B. A. Carreras, D. E. Newman, and I. Dobson, North American blackout time series statistics and implications for blackout risk, *IEEE Trans. Power Syst.* **31**, 4406 (2016).
- [19] I. Dobson, B. A. Carreras, V. E. Lynch, and D. E. Newman, Complex systems analysis of series of blackouts: Cascading failure, critical points, and self-organization, *Chaos* **17**, 026103 (2007).
- [20] R. Weron and I. Simonsen, in *Practical Fruits of Econophysics*, edited by H. Takayasu (Springer Tokyo, Tokyo, 2006), p. 215.
- [21] G. Ancell, C. Edwards, and V. Krichtal, in *Electricity Engineers Association 2005 Conference "Implementing New Zealand's Energy Options"* (Auckland, New Zealand, 2005).
- [22] X. Weng, Y. Hong, A. Xue, and S. Mei, Failure analysis on China power grid based on power law, *J. Control. Theory Appl.* **4**, 235 (2006).
- [23] J. Chen, J. Thorp, and M. Parashar, in *Proceedings of the 34th Annual Hawaii International Conference on System Sciences* (IEEE, Maui, HI, USA, 2001), p. 738.
- [24] J. Ø. H. Bakke, A. Hansen, and J. Kertész, Failures and avalanches in complex networks, *Europhys. Lett.* **76**, 717 (2006).
- [25] Å. J. Holmgren and S. Molin, Using disturbance data to assess vulnerability of electric power delivery systems, *J. Infrastruct. Syst.* **12**, 243 (2006).
- [26] B. A. Carreras, J.-M. Reynolds-Barredo, I. Dobson, and D. E. Newman, in *52th Hawaii International Conference on System Sciences* (Grand Wailea HI, USA, 2019), <https://aisel.aisnet.org/hicss-52/>.
- [27] M. Rosas-Casals and R. Solé, Analysis of major failures in Europe's power grid, *Int. J. Electr. Power Energy Syst.* **33**, 805 (2011).
- [28] S. Kancherla and I. Dobson, Heavy-tailed transmission line restoration times observed in utility data, *IEEE Trans. Power Syst.* **33**, 1145 (2018).
- [29] It has to be noted that most data providers do not distinguish between outage and restoration processes in their openly published datasets; thus, from herein we refer to outage duration as the time passing between the deenergization and the reenergization of a power system component.
- [30] The spectral analysis of the outage duration times is less clear. For certain databases, one cannot see a crossover between random and PL correlations, if the temporal resolution is low.
- [31] ENTSO-E, Unavailability of Production and Generation Units, <https://transparency.entsoe.eu/outage-domain/r2/unavailabilityOfProductionAndGenerationUnits/show> (Dates span from December 11, 2014 to July 10, 2022), data downloaded through the provided API: <https://transparency.entsoe.eu/content/static/content/Static%20content/web%20api/Guide.html>, which can be conveniently accessed via the "entsoe-py" client: <https://github.com/EnergieID/entsoe-py>.
- [32] California ISO - Curtailed and Non-Operational Generators, <http://www.aiso.com/market/Pages/OutageManagement/CurtailedandNonOperationalGenerators.aspx> (Dates span from June 17, 2021 to July 25, 2022).
- [33] Expost Information On Unplanned Unavailability of Generation Units - MAVIR - Magyar Villamosenergia-ipari Átviteli Rendszerirányító Zrt., <https://www.mavir.hu/web/mavir-en/expost-information-on-unplanned-unavailability-of-generation-units> (Dates span from September 8, 2010 to June 29, 2022).
- [34] GME Inside Information Platform, Production Unavailability, <https://pip.ipex.it/PipWa/Front/#/PowerUmms> (Dates from December 31, 2015 to July 7, 2017).
- [35] Bonneville Power Administration Outage & Reliability Reports, <https://transmission.bpa.gov/Business/Operations/Outages/> (Dates span from January 1, 1988 to April 6, 2022).
- [36] AESO Historical Transmission Outages Data 2013–2019, <https://www.aeso.ca/market/market-and-system-reporting/data-requests/historical-transmission-outages-data/> (Dates span from April 28, 2013 to November 4, 2019).
- [37] ENTSO-E, Unavailability of Transmission Grid, <https://transparency.entsoe.eu/outage-domain/r2/unavailabilityInTransmissionGrid/show> (Dates span from December 11, 2014 to July 10, 2022), see [31] for data collection details.
- [38] H. Bálint, S. Deng, G. Odor, and J. Kelling, Raw outage data for this paper, <https://doi.org/10.5281/zenodo.8055548> (2023).
- [39] B. A. Carreras, D. E. Newman, I. Dobson, and A. Poole, in *Proceedings of the 33rd Annual Hawaii International Conference on System Sciences* (IEEE, Maui, HI, USA, 2000), p. 6.
- [40] G. Ódor and B. Hartmann, Power-law distributions of dynamic cascade failures in power-grid models, *Entropy* **22**, 666 (2020).
- [41] T. Nesti, F. Sloothak, and B. Zwart, Emergence of Scale-Free Blackout Sizes in Power Grids, *Phys. Rev. Lett.* **125**, 058301 (2020).
- [42] B. Hartmann *et al.*, Heterogeneity of the European grids: Nodal behaviour, edge weight, frequency analysis, (to be published 2023).
- [43] A. Clauset, C. R. Shalizi, and M. E. Newman, Power-law distributions in empirical data, *SIAM Rev.* **51**, 661 (2009).
- [44] From Eq. (1), the probability density diverges as  $x \rightarrow 0$ , so a lower bound is also mandatory mathematically.
- [45] S. M. Harvey, W. W. Hogan, and T. Schatzki, in *Toulouse Conference paper* (Toulouse, France, 2004), [https://scholar.harvard.edu/whogan/files/harvey\\_hogan\\_schatzki\\_toulouse\\_010204.pdf](https://scholar.harvard.edu/whogan/files/harvey_hogan_schatzki_toulouse_010204.pdf).
- [46] H. Wu, X. Meng, M. M. Danziger, S. P. Cornelius, H. Tian, and A.-L. Barabási, Fragmentation of outage clusters during the recovery of power distribution grids, *Nat. Commun.* **13**, 7372 (2022).
- [47] For both  $S(t)$  and  $I(t)$ , we had first excluded events recorded at 1/4, 1/2, 3/4 h and whole hours to eliminate any artifacts in outage bookkeeping time, if many events were recorded at such time points.
- [48] R. G. Brown and P. Y. Hwang, *Introduction to Random Signals and Applied Kalman Filtering: with MATLAB Exercises and Solutions* (Wiley, New York, NY, USA, 2012).

- [49] S. Murphy, J. Apt, J. Moura, and F. Sowell, Resource adequacy risks to the bulk power system in North America, *Appl. Energy* **212**, 1360 (2018).
- [50] S. Murphy, F. Sowell, and J. Apt, A time-dependent model of generator failures and recoveries captures correlated events and quantifies temperature dependence, *Appl. Energy* **253**, 113513 (2019).
- [51] G. J. McLachlan, S. X. Lee, and S. I. Rathnayake, Finite mixture models, *Annu. Rev. Stat. Appl.* **6**, 355 (2019).
- [52] R. B. Duffey, Power restoration prediction following extreme events and disasters, *Int. J. Disaster Risk Sci.* **10**, 134 (2019).
- [53] C. J. Zapata, S. C. Silva, H. I. Gonzalez, O. L. Burbano, and J. A. Hernandez, in *2008 IEEE/PES Transmission and Distribution Conference and Exposition: Latin America* (IEEE, Bogota, Columbia, 2008), p. 1.
- [54] P. Bak, *How Nature Works: The Science of Self-Organized Criticality* (Springer New York, New York, NY, USA, 2013).
- [55] H. Stanley, L. Amaral, S. V. Buldyrev, P. Gopikrishnan, V. Plerou, and M. Salinger, Self-organized complexity in economics and finance, *PNAS* **99**, 2561 (2002).
- [56] G. Ódor, *Universality in Nonequilibrium Lattice Systems: Theoretical Foundations* (World Scientific Publishing Co., Singapore, Singapore, 2008).
- [57] R. Dickman, A. Vespignani, and S. Zapperi, Self-organized criticality as an absorbing-state phase transition, *Phys. Rev. E* **57**, 5095 (1998).
- [58] R. Dickman, M. A. Muñoz, A. Vespignani, and S. Zapperi, Paths to self-organized criticality, *Braz. J. Phys.* **30**, 27 (2000).
- [59] A. Aharony and D. Stauffer, *Introduction to Percolation Theory* (Taylor & Francis, London, 2003).
- [60] S. R. Broadbent and J. M. Hammersley, Percolation processes, *Math. Proc. Camb. Philos. Soc.*, **53**, 629 (1957).
- [61] F. Van Wijland, K. Oerding, and H. Hilhorst, Wilson renormalization of a reaction–diffusion process, *Physica A* **251**, 179 (1998).
- [62] K. Zhou, I. Dobson, Z. Wang, A. Roitershtein, and A. P. Ghosh, A Markovian influence graph formed from utility line outage data to mitigate large cascades, *IEEE Trans. Power Syst.* **35**, 3224 (2020).
- [63] E. Frey, U. C. Täuber, and F. Schwabl, Crossover from isotropic to directed percolation, *Phys. Rev. E* **49**, 5058 (1994).
- [64] Z. Zhou, J. Yang, R. M. Ziff, and Y. Deng, Crossover from isotropic to directed percolation, *Phys. Rev. E* **86**, 021102 (2012).
- [65] D. J. Korchinski, J. G. Orlandi, S.-W. Son, and J. Davidsen, Criticality in Spreading Processes without Timescale Separation and the Critical Brain Hypothesis, *Phys. Rev. X* **11**, 021059 (2021).
- [66] Numerical analysis showed that, in the presence of such composite reactions, the cascade size and duration distribution exponents crossover to larger values on complex networks [80,81] for larger avalanche sizes and durations. This agrees and may explain our power-law fitting results for the failure durations, where we see a crossover around  $t_c \simeq 24$  h from smaller to bigger  $\tau_T$  exponents. Note that in the databases the outage times are rounded to 1-min or 1-h slots, so shorter-time results may not be reliable.
- [67] M. Henkel, H. Hinrichsen, and S. Lübeck, *Non-Equilibrium Phase Transitions* (Springer, Dordrecht, The Netherlands, 2008), Vol. 1.
- [68] S. Lübeck, Universal Behavior of Crossover Scaling Functions for Continuous Phase Transitions, *Phys. Rev. Lett.* **90**, 210601 (2003).
- [69] M. Henkel and M. Pleimling, *Non-Equilibrium Phase Transitions* (Springer, Dordrecht, The Netherlands, 2010), Vol. 2.
- [70] R. B. Griffiths, Nonanalytic Behavior Above the Critical Point in a Random Ising Ferromagnet, *Phys. Rev. Lett.* **23**, 17 (1969).
- [71] M. A. Muñoz, R. Juhász, C. Castellano, and G. Ódor, Griffiths Phases on Complex Networks, *Phys. Rev. Lett.* **105**, 128701 (2010).
- [72] J. Doyle and J. M. Carlson, Power Laws, Highly Optimized Tolerance, and Generalized Source Coding, *Phys. Rev. Lett.* **84**, 5656 (2000).
- [73] A. Vinogradov, V. Bolshev, A. Vinogradova, M. Jasiński, T. Sikorski, Z. Leonowicz, R. Goño, and E. Jasińska, Analysis of the power supply restoration time after failures in power transmission lines, *Energies* **13**, 2736 (2020).
- [74] S. M. Harvey, W. W. Hogan, and T. Schatzki, *A hazard rate analysis of Mirant's generating plant outages in California (Jan-04)*, Working Paper Series (Harvard University, John F. Kennedy School of Government, 2005).
- [75] T.-W. Kim, Y. Chang, D.-W. Kim, and M.-K. Kim, Preventive maintenance and forced outages in power plants in Korea, *Energies* **13**, 3571 (2020).
- [76] L. Laurson, M. J. Alava, and S. Zapperi, Power spectra of self-organized critical sandpiles, *J. Stat. Mech: Theory Exp.* **2005**, L11001 (2005).
- [77] A. K. Kalashyan, M. Buiatti, and P. Grigolini, Ergodicity breakdown and scaling from single sequences, *Chaos Solit. Fractals* **39**, 895 (2009).
- [78] J. A. Bonachela and M. A. Muñoz, Confirming and extending the hypothesis of universality in sandpiles, *Phys. Rev. E* **78**, 041102 (2008).
- [79] I. Dobson, Estimating the propagation and extent of cascading line outages from utility data with a branching process, *IEEE Trans. Power Syst.* **27**, 2146 (2012).
- [80] C. Moore and M. E. J. Newman, Exact solution of site and bond percolation on small-world networks, *Phys. Rev. E* **62**, 7059 (2000).
- [81] R. Cohen, D. ben Avraham, and S. Havlin, Percolation critical exponents in scale-free networks, *Phys. Rev. E* **66**, 036113 (2002).